Part II DETAILED DISCUSSION

Part II DETAILED DISCUSSION

Chapter 1 Analysis of the Existing Data

1.1 Organizations to supply the existing data

The existing data were collected from Geological Information Center, Mineral Resources Authority of Mongolia (GIC, MRAM). All the data of the geological survey and exploration of mineral resources conducted in Mongolia during the time when the country was a socialist state, as well as the data obtained by surveys and exploration conducted by Mongolian government after democratization of the country in 1990 are stored at GIC. Only one set of the reports and associated drawings is original. Although access to them is permitted to Mongolians and foreigners, taking them out of GIC is prohibited. We have brought copies of necessary maps and reports for the survey out of Mongolia with special permission from MRAM. Also copies of the existing data concerning the Erdenet mine and its surroundings were assigned by Erdenet Mining Corporation.

Documents and papers were collected from GIC and through JICST (Japan Information Center of Science and Technology), and those considered to be important were translated from Russian to English (see tables in Appendix).

1.2 Kinds of the existing data

Since the existing data were in a wide variety, they were classified into the following categories. Details of the data were compiled into lists per category (see tables in Appendix). Areas which the data cover are basically included in the Central North area of Monaolia.

- Scientific and technical papers, reports and books (Appendix Table A-1)
- Data on ore deposits, mineral deposits and mineral occurrences (Appendix Table A-2, A-3)
  The list covers 500 deposits and occurrences located in the survey area.
- Topographic map of 1:500,000 : 6 sheets (Appendix Table A-4)
  Colored geography is given on the elevation contour. A border, main roads, names of major municipalities, names of rivers, mountains and lakes are described in Mongolian language.
- Topographic map of 1:100,000 : 19 sheets (Appendix Table A-4)
  Black and white. Elevation contour, names of major municipalities, rivers and mountains are described in Mongolian language.
- Geological map of 1:1,000,000 : 2 sheets (Appendix Table A-5)
- Geological map of 1:500,000 : 1 sheet (Appendix Table A-5)
  This was produced jointly with the former USSR in 1900s
- Mineral resources map of 1:500,000 : 6 sheets including legend (Appendix Table A-5)
- Geological map of 1:200,000 and a report (Appendix Table A-5, Figure II-1-1)

- Geological map of 1:50,000 and a report (Appendix Table A-5, Figure II-1-2)
  These sets consist of maps and a report (in Russian) jointly produced before 1989 with the former USSR at the time of the joint survey, and maps and a report (in Mongolian) produced from 1990 onward at the time of the survey by Mongolia alone. The supplementary report consists of three chapters, i.e. Chapter 1: Geological Structure, Chapter 2: Minerals and Deposits, and Chapter 3: Summary and Future Outlook. Only Chapter 3 was translated into English in this project.
- Geological maps around mineral occurrences: 29 occurrences (Appendix Table A-6)
- Geological map and geochemical / geophysical exploration results of the Erdenet mine and its vicinity (Appendix Table A-7)
  Black and white as well as colored plans and profiles in various reduced scales which were produced mainly in 1980s.
- Map and list of mining area (Table II-1-7)
- Summary of the supplementary report on geophysical exploration (Appendix Table A-8, Figure II-1-3)
  Electric method (resistivity, IP), electro-magnetics, magnetics, airborne magnetics and radiometrics.

1.3 Analysis of the existing data

- Before the field survey
  Occurrences with high-grade copper and gold (Standard Cu≧0.02 %, Au≧0.1 g/t) were selected from the list of ore deposits, mineral deposits and mineral occurrences (Appendix Table A-2, A-3). The sites subject to ground truth were further determined from among those occurrences.
- During the field survey
  The data (geological, geochemical and geophysical maps) on surroundings of the ground truth sitets were examined before execution of the field survey so that its efficiency might be high.

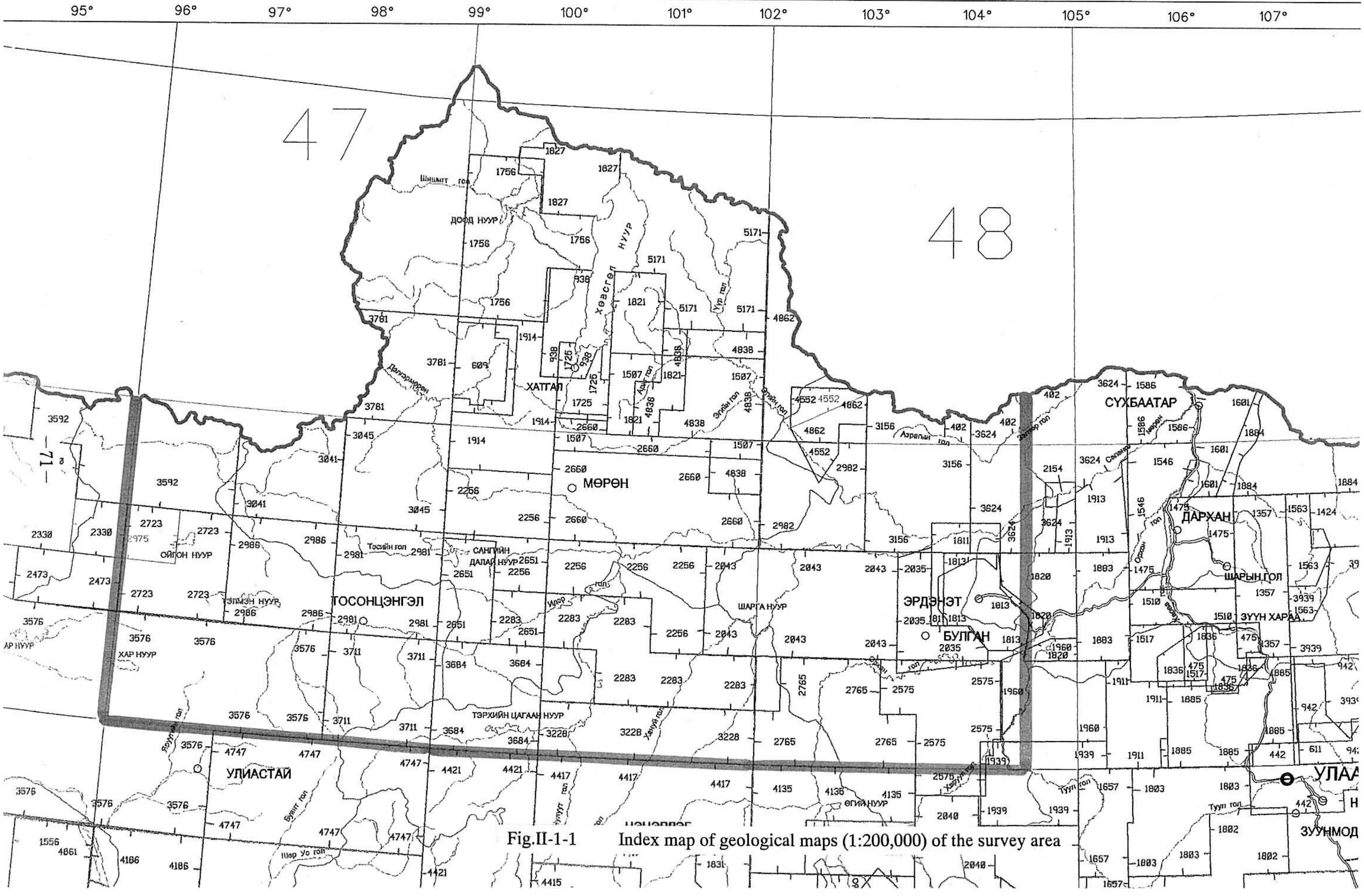

Fig.II-1-1 Index map of geological maps (1:200,000) of the survey area

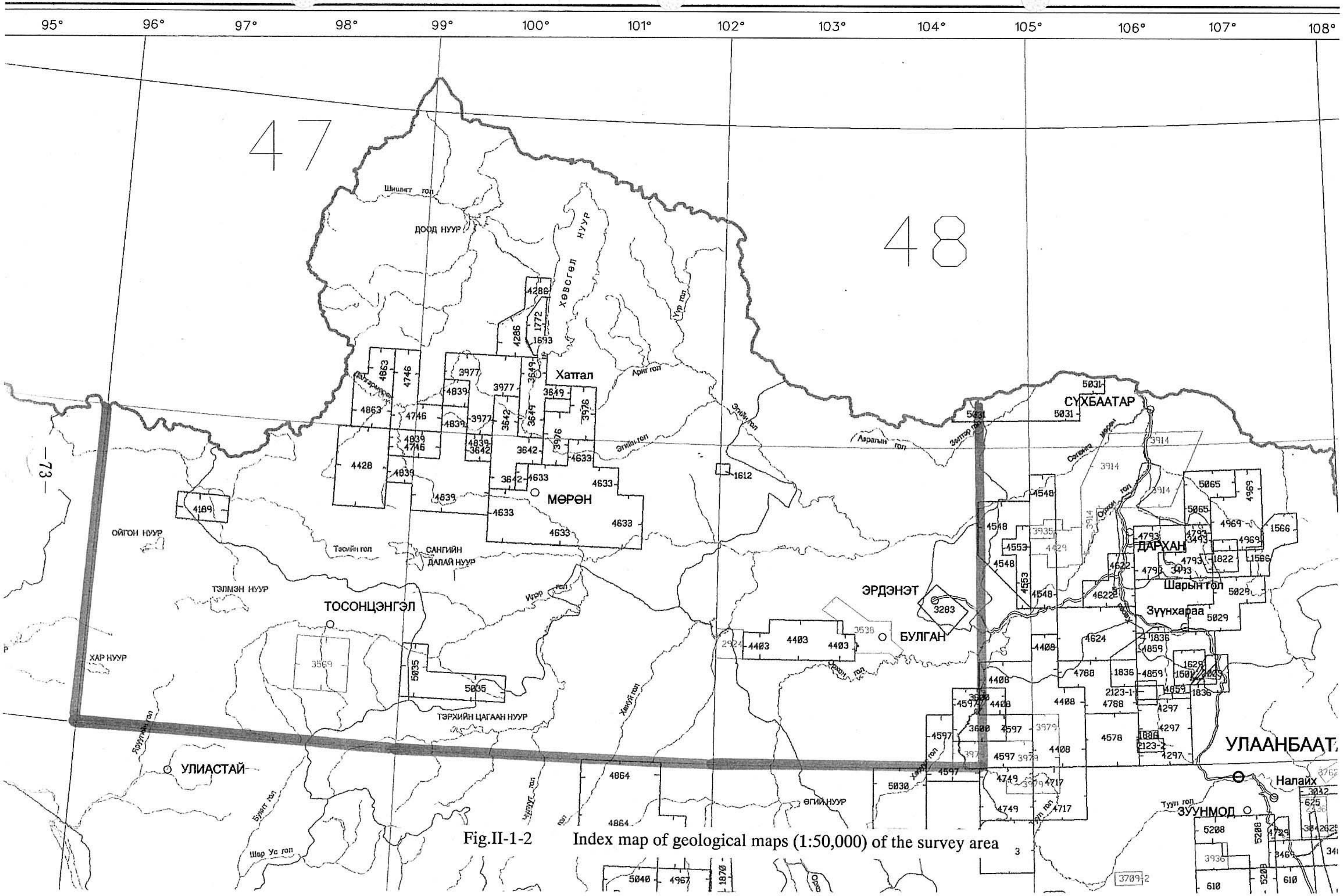

Fig.II-1-2 Index map of geological maps (1:50,000) of the survey area

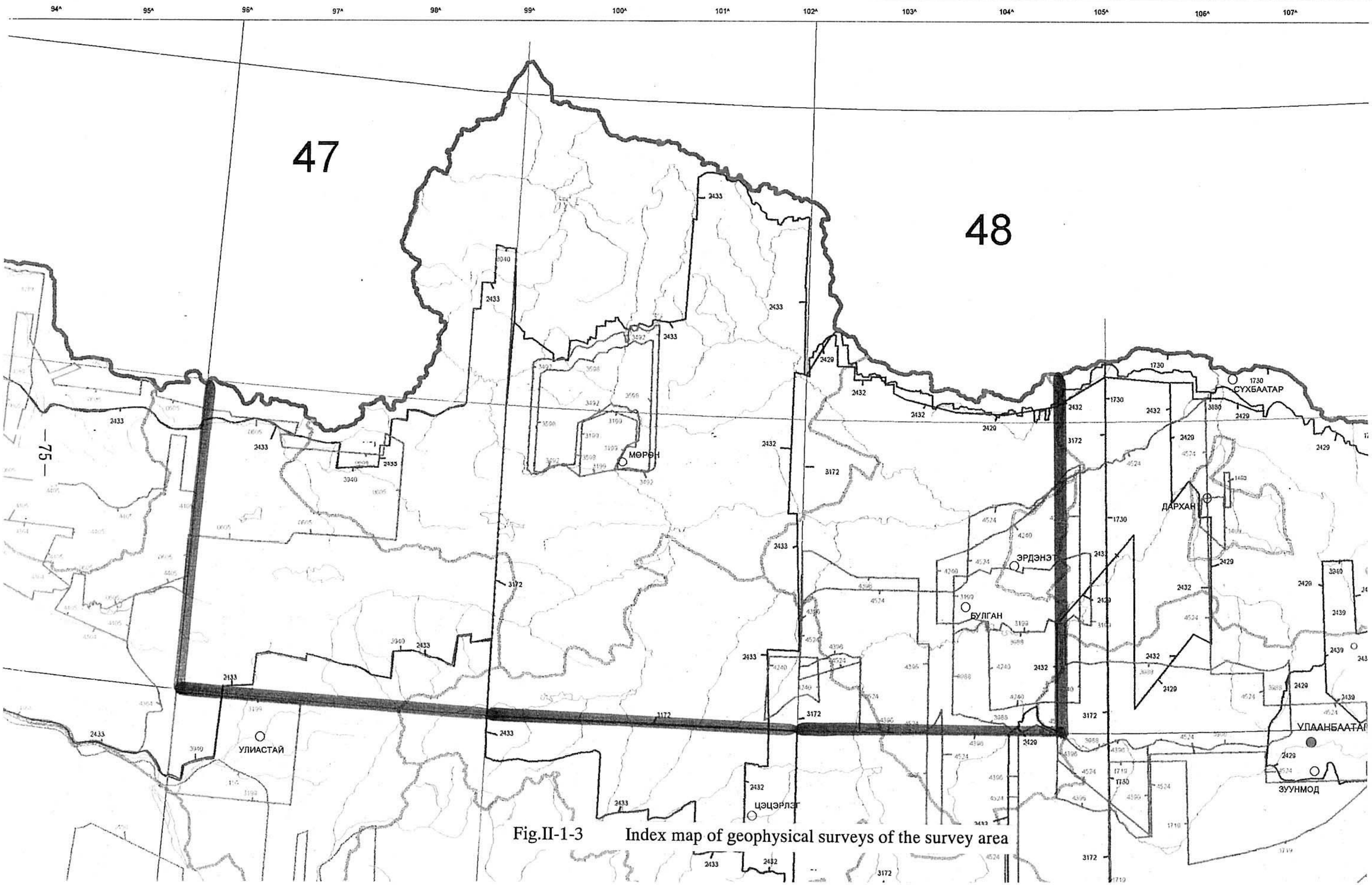

Fig.II-1-3 Index map of geophysical surveys of the survey area

Chapter 2 Analysis of Satellite Image

2.1 Processing and production of image

2.1.1 Introduction

(1) Purpose

Purpose was to produce digital mosaic images using JERS-1/SAR data for the central north area of Mongolia ranging from 48° to 52° N latitude and from 96° to 105° E longitude (excluding the area belonging to Russian Federation). Size of a unit of mosaic image was 1° in N-S by 1.5° E-W. The mosaic image of the whole area was also produced.

(2) Method

Method of processing and proeuction of image were described as follows:

- Bit conversion, trend correction, calculation of relative positions, conjunction of scenes and density adjustment were conducted on JERS-1/SAR data to prepare digital mosaic images.
- By comparing digital mosaic images with the topographic map, geographical coordinate systems were assigned to the images. Then, the images were cut out for each unit of sheet (1° in N-S by 1.5° in S-W).
- Individual sheet was stitched with each other to produce the mosaic image of the whole area.

(3) Outline of the area

The area is located in the central north area of Mongolia, ranging from 48° to 52° N latitude and from 96° to 105° E longitude (excluding the area belonging to Russian Federation), ranging approximately 250,000 km^2 (Figure II-2-1). The area corresponds to the west of Lake Baikal. While the southern part includes many steppes and swamps, the northern part consists of mountains of higher than 3,000 m above the sea level.

2.1.2 Satellite data

JERS-1/SAR data to cover the area consists of 141 scenes when each scene is expressed as a square. However, since some part of the 141 scenes belongs to Russia, the actual area inside Mongolia would be in a shape of a convex, that is its northwest and northeast corners lacking from a whole square. Therefore, a total of 130 scenes were actually used to prepare the entire mosaic images (Table II-2-1 and Figure II-2-2).

2.1.3 Hardware and software

The following equipments to produce images were employed:
- Hardware: HP9000 series J200 (OS: HP-UX 10.01)
- Software : ERDAS Imagine (Ver 8.2) and in-house software for image processing.

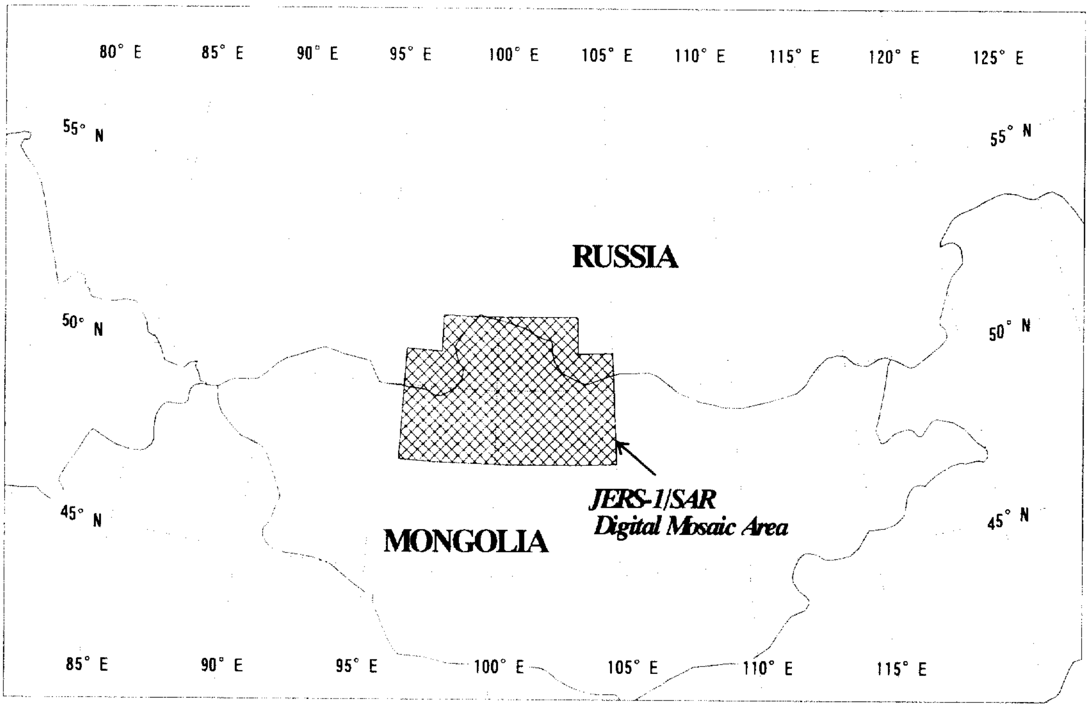

Fig. II-2-1 Locality of satellite image

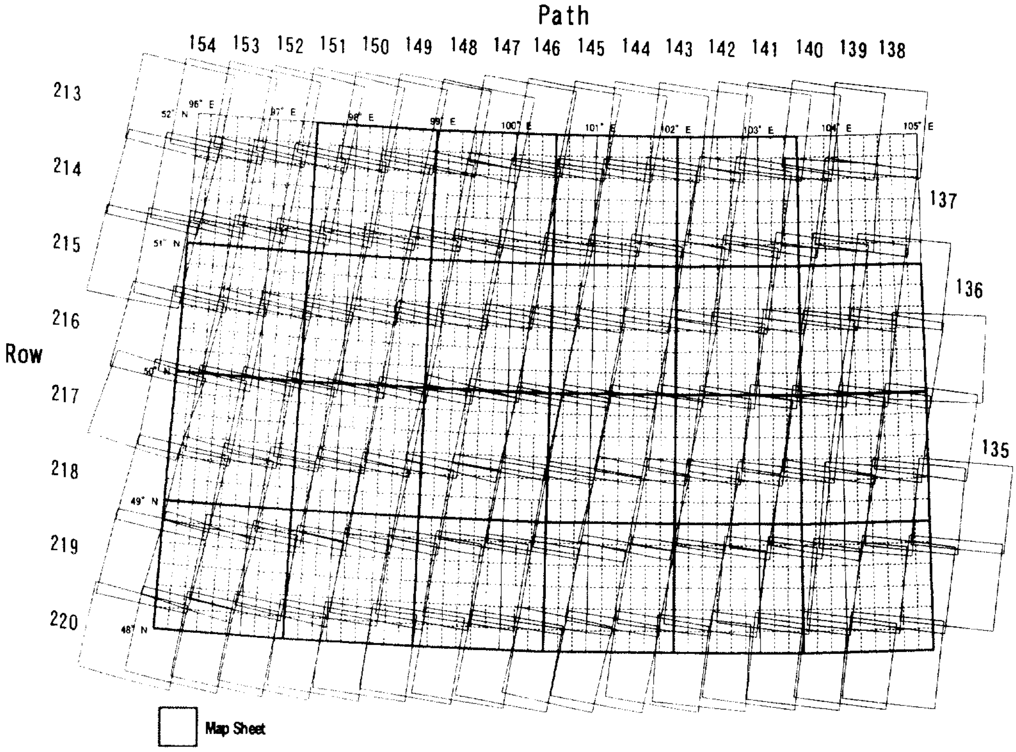

Fig. II-2-2 Index map of JERS-1/SAR data

Table II-2-1 List of JERS-1/SAR data

Path	Row	Date	N/U
135	218	1997/04/24	※
	219	1997/04/24	
	220	1997/04/25	
136	216	1997/04/25	
	217	1997/04/25	
	218	1997/04/25	
	219	1997/04/25	
	220	1997/04/26	
137	215	1997/04/26	
	216	1997/04/26	
	217	1997/04/26	
	218	1997/04/26	
	219	1997/04/26	
	220	1997/04/27	
138	213	1997/04/27	※
	214	1997/04/27	※
	215	1997/04/27	
	216	1997/04/27	
	217	1997/04/27	
	218	1997/04/27	
	219	1997/04/27	
	220	1995/07/08	
139	213	1994/01/26	※
	214	1995/07/08	
	215	1995/07/08	
	216	1995/07/08	
	217	1995/07/08	
	218	1995/07/08	
	219	1995/07/08	
	220	1997/04/29	
140	213	1997/04/29	
	214	1997/04/29	
	215	1997/04/29	
	216	1997/04/29	
	217	1997/04/29	
	218	1997/04/29	
	219	1997/04/29	
	220	1993/05/09	
141	213	1995/01/15	
	214	1993/05/09	
	215	1993/05/09	
	216	1993/05/09	
	217	1993/05/09	
	218	1993/05/09	
	219	1997/04/30	
	220	1997/05/01	

Path	Row	Date	N/U
142	213	1997/05/01	
	214	1997/05/01	
	215	1997/05/01	
	216	1997/05/01	
	217	1997/05/01	
	218	1997/05/01	
	219	1997/05/01	
	220	1997/05/02	
143	213	1997/05/02	
	214	1997/05/02	
	215	1997/05/02	
	216	1997/05/02	
	217	1997/05/02	
	218	1997/05/02	
	219	1997/05/02	
	220	1997/05/03	
144	213	1997/05/03	
	214	1997/05/03	
	215	1997/05/03	
	216	1997/05/03	
	217	1997/05/03	
	218	1997/05/03	
	219	1997/05/03	
	220	1997/05/04	
145	213	1994/02/01	
	214	1994/02/01	
	215	1994/02/01	
	216	1994/02/01	
	217	1994/02/01	
	218	1994/02/01	
	219	1994/02/01	
	220	1994/02/02	
146	213	1994/02/02	
	214	1994/02/02	
	215	1994/02/02	
	216	1994/02/02	
	217	1994/02/02	
	218	1994/02/02	
	219	1994/02/02	
	220	1994/02/02	
147	213	1997/05/06	
	214	1997/05/06	
	215	1997/05/06	
	216	1997/05/06	
	217	1997/05/06	
	218	1997/05/06	
	219	1997/05/06	
	220	1997/05/07	

Path	Row	Date	N/U
148	213	1997/05/07	
	214	1997/05/07	
	215	1997/05/07	
	216	1997/05/07	
	217	1997/05/07	
	218	1997/05/07	
	219	1997/05/07	
	220	1997/05/08	
149	213	1997/05/08	
	214	1997/05/08	
	215	1997/05/08	
	216	1997/05/08	
	217	1997/05/08	
	218	1997/05/08	
	219	1997/05/08	
	220	1997/05/09	
150	213	1997/05/09	
	214	1997/05/09	
	215	1997/05/09	
	216	1997/05/09	
	217	1997/05/09	
	218	1997/05/09	
	219	1997/05/09	
	220	1997/05/10	
151	213	1997/05/10	
	214	1997/05/10	
	215	1997/05/10	
	216	1997/05/10	
	217	1997/05/10	
	218	1997/05/10	
	219	1997/05/10	
	220	1997/05/11	
152	213	1997/05/11	※
	214	1997/05/11	※
	215	1997/05/11	
	216	1997/05/11	
	217	1997/05/11	
	218	1997/05/11	
	219	1997/05/11	
153	213	1997/05/12	※
	214	1997/05/12	※
	215	1997/05/12	
	216	1997/05/12	
	217	1997/05/12	
154	213	1997/05/13	※
	214	1997/05/13	※
	215	1997/05/13	※

Mark ※ in N/U column shows JERS-1/SAR data that is not used for production of the mosaic image

2.1.4 Data processing

(1) Production of digital mosaics

Figure II-2-3 shows a flow of producing digital mosaic images. Mosaic wsd produced for a sheet of 1° in N-S by 1.5° in E-W. In order to acquire basic information of the data, a histogram of 16 bit data was output for all the data, and condition of the images was checked through visual inspection.

(a) Bit conversion

Since JERS-1/SAR level 2.1 data were provided in 16 bits with marks, the data were converted into 8 bit data after calculation of the basic statistic quantity. Since 16 bit data themselves represented their physical quantities, if individual scenes were converted into 8 bits in different width, relative relation of physical quantities within their original data would be damaged. This would appear in difference in gray level among images when they are stitched. Therefore it is better to stretch all the data in the same width in converting them into 8 bits. When conducting bit conversion, taking into consideration that the form of histogram of the data in 16 bits is unsymmetry, we compared typical histogram representing areas from swamps to mountains with each other. Then the stretching width was determined to be the range in which image characteristics of the original data remains as much as possible over these areas. The stretch width used was from 0 to 2800.

(b) Trend correction

In JERS-1/SAR image there is a trend which is in parallel with the azimuth direction (direction of the satellite orbit) and changes toward direction of the range (direction of radar irradiation). The trend was extracted from the image, and after obtaining difference between average of all the data and the trend, the difference was subtracted from the original image. When extracting the trend, image data which is not occupied by many lakes and mountains, that is parts with little variation, were employed. If it is impossible to extract trend from the image, trend extracted from another image is used for correction of the image.

(c) Calculation of relative positions

To produce satellite image mosaics in general, Ground Control Point (GCP) was established for each scene, and geographical coordinate systems were assigned to them before they were stitched. However, in case that it is difficult to decide GCP because topographic map of the relevant area is not accurate or surface characteristics is lacking, the effect is focusing on a part of its mosaic image resulting in distortion and accuracy in its conjunction is excessively degraded. In some cases due to deflection of the satellite orbit, positional shift happens between JERS-1/SAR images which are projected onto the UTM coordinate. Therefore, we applied a method of calculating relative positions among images as rotational component, and by rotating the images to avoid their possible positional changes. Here, positions were adjusted through mutual rotation of images whose process is shown in Figure II-2-4 so that possible changes might not be focused on a certain point.

First, image data of four scenes adjacent to one another were handled in a suite and their mutual rotating angles α_{AB}, α_{BC}, α_{CD} and α_{DA} were obtained. Then, 1/4 of θ, the final difference in

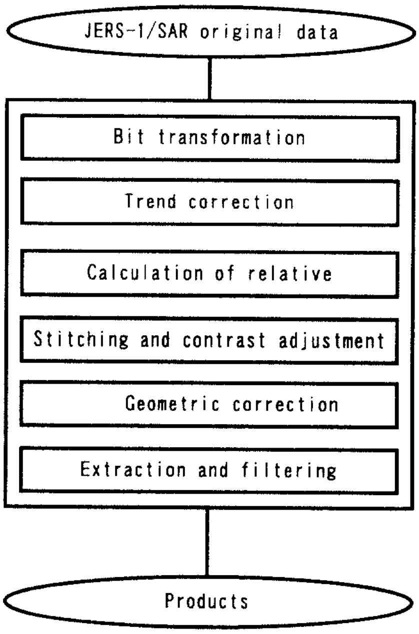

Fig. II-2-3 Flow chart of producing JERS-1/SAR mosaic image

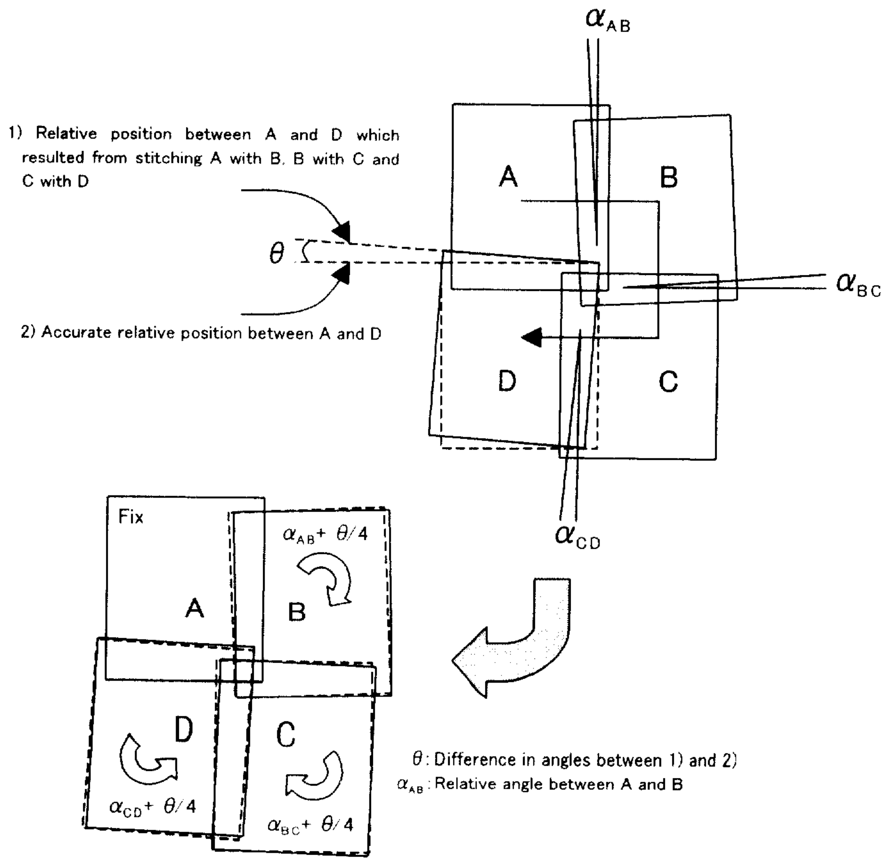

Fig. II-2-4 Process of stitching 4 scenes of JERS-1/SAR data angles arising from the rotation of the images was assigned to the four scenes, and individual image data were rotated in accordance with the resulting angles. In consequence, 1/4 of θ, the difference in angles obtained through assignment to the four scenes becomes an error arising from stitches of the four scenes.

(d) Conjunction of scenes and adjustment of gray level

The image data rotated by calculating their relative positions were conjugated in accordance with the relative positions obtained. Because there is difference in gray levels because of time gap of the data acquisition, the images were conjugated after adjusting the gray levels. For adjustment of gray levels, the statistics of levels were determined on the portion where the conjugated scenes overlapped, and average value and standard deviation of each scene was modified to be consistent.

(2) Geometric correction of mosaics

In order to allocate geographical coordinate to the produced mosaics, geometric correction was conducted by comparing TM images with the topographic map data. Since topography of this area in scale of 1:500,000 of Tactical Pilotage Chart (TPC) was digitized, GCPs were determined based on these data and then geometric correction was done. The GCPs were 10 to 12 in number per one sheet of the image. We set as many GCPs as possible to be located in the periphery of a sheet of the image, and a few inside the image, and tried GCPs to keep uniform distance with each other.

For geometric correction, the third affine transformation was used to decrease the total RMS errors to be less than ten. In order that the statistics of the original data is not demolished, resampling was conducted using the nearest method, and the final pixel size was decided to be12.5 m, the same as that of the original data.

The coordinate used was the UTM (Universal Transverse Melcatol) projection and "Krasovsky" was used for ellipsoid. In the UTM projection, a zone is set up with the width of three degrees of longitude in E-W direction from central meridian. Since 102° E longitude was a boundary between Zone 47 and Zone 48 in this area, 15 images located in the west of 102° E longitude were determined to be in Zone 47, and 7 images located to the east from there were determined to be in Zone 48.

(3) Cutting out and filtering

The mosaics to which the UTM coordinate were allocated were cut out in 1° in N - S by 1.5° in E-W. In the trimming, an overlapped portion of 5′ each was left from the northwest corner to the northern and western directions, and from the southeast corner to the eastern and southern directions. When outputting images, a median filter of 3 pixels by 3 pixels was used to prevent roughness of the surface affected by speckle noise peculiar to SAR data so that detailed information might be visible. A print of 1:200,000 scale was output with titles and scales indicated.

Name given to an individual image was derived from major municipalities or lakes located in the area of the image. Table II-2-2 and Figure II-2-5 show a list of individual images and index map respectively, and Figure II-2-6 shows an example of the output of the image.

(4) Preparation of mosaic image of the entire area

In addition to the images of 1° (N-S) by 1.5° (E-W), the mosaic image of the entire area was

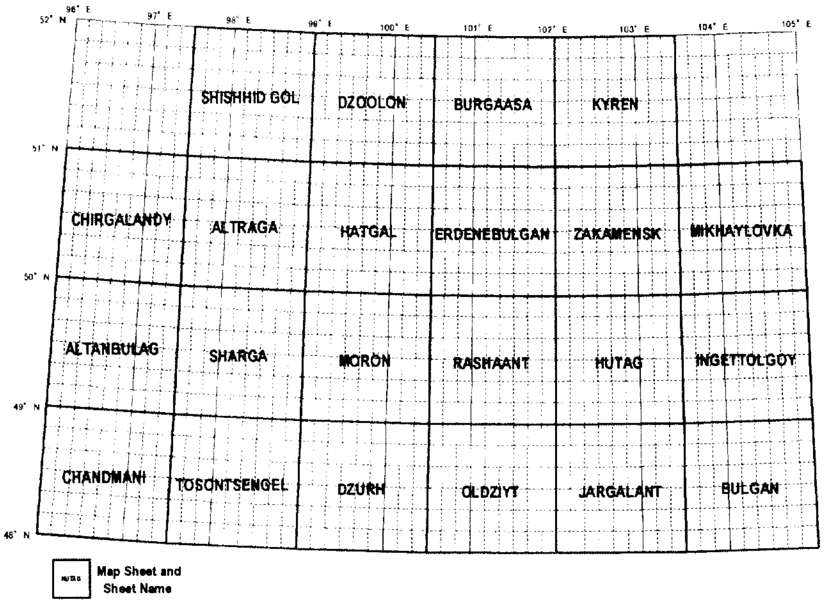

Fig. II-2-5 Index map of JERS-1/SAR mosaic images

Table II-2-2 List of JERS-1/SAR mosaic images

Image Unit	*Corner of the left upper side*		*Corner of the right upper side*		*UTM Zone*
	Longitude	*Latitude*	*Longitude*	*Latitude*	
SHISHHID GOL	N97°30'	E52°00'	N99°00'	E51°00'	N47
DZÖÖLÖN	N99°00'	E52°00'	N100°30'	E51°00'	N47
BURGAASA	N100°30'	E52°00'	N102°00'	E51°00'	N47
KYREN	N102°00'	E52°00'	N103°30'	E51°00'	N48
CHIRGALANDY	N96°00'	E51°00'	N97°30'	E50°00'	N47
ALTRAGA	N97°30'	E51°00'	N99°00'	E50°00'	N47
HATGAL	N99°00'	E51°00'	N100°30'	E50°00'	N47
ERDENEBULGAN	N100°30'	E51°00'	N102°00'	E50°00'	N47
ZAKAMENSK	N102°00'	E51°00'	N103°30'	E50°00'	N48
MIKHAYLOVKA	N103°30'	E51°00'	N105°00'	E50°00'	N48
ALTANBULAG	N96°00'	E50°00'	N97°30'	E49°00'	N47
SHARGA	N97°30'	E50°00'	N99°00'	E49°00'	N47
MÖRÖN	N99°00'	E50°00'	N100°30'	E49°00'	N47
RASHAANT	N100°30'	E50°00'	N102°00'	E49°00'	N47
HUTAG	N102°00'	E50°00'	N103°30'	E49°00'	N48
INGETTOLGOY	N103°30'	E50°00'	N105°00'	E49°00'	N48
CHANDMANI	N96°00'	E49°00'	N97°30'	E48°00'	N47
TOSONTSENGEL	N97°30'	E49°00'	N99°00'	E48°00'	N47
DAÜRH	N99°00'	E49°00'	N100°30'	E48°00'	N47
ÖLDZIYT	N100°30'	E49°00'	N102°00'	E48°00'	N47
JARGALANT	N102°00'	E49°00'	N103°30'	E48°00'	N48
BULGAN	N103°30'	E49°00'	N105°00'	E48°00'	N48

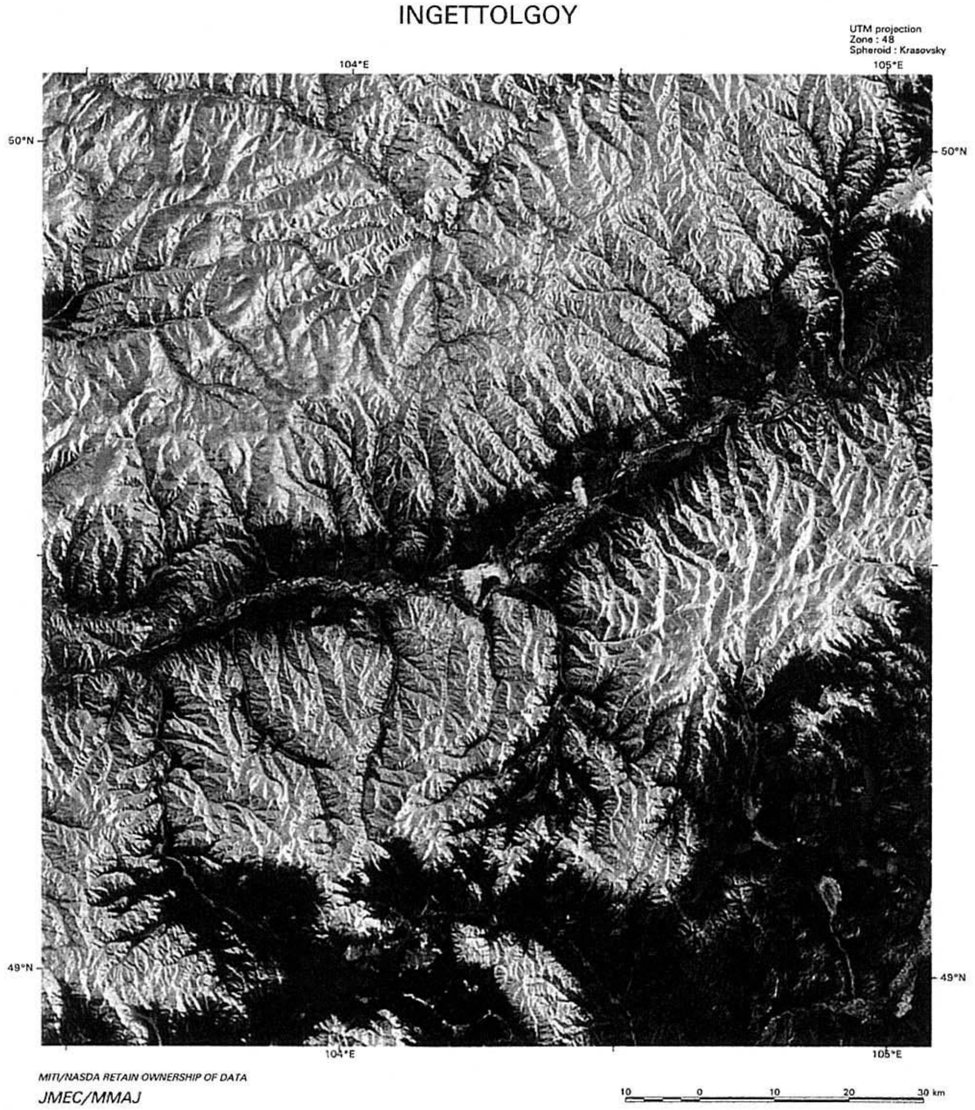

Fig.II-2-6 Example of 1° ×1.5° JERS-1/SAR mosaic image (INGETTOLGOY) also produced. The coordinate was already allocated to each image. However, since the images extended over two zones of the UTM coordinate, it was necessary to unify the coordinate system in preparing the mosaic image of the entire area. It was possible to unify them to either of the two UTM zones. However, in areas of high latitudes like this area, the more they are away from the central meridian, the more distorted the coordinate would be. Therefore, Lambert's conformal projection method was applied which is suitable to project areas of medium latitudes. A print 1:1,000,000 scale was output with titles nad scales indicated, etc. Figure II-2-7 shows the mosaic image of the entire area.

2.2 Analysis of the image

2.2.1 Outline

The area covered for analysis of Landsat TM image was located in the northern central part of Mongolia ranging from 48° to 52° N latitude and from 100° 30′ to 105° E Lngitude, within the border with Russian Federation in the northern end. The area is situated to the west of the capital Ulaanbaatar including Khovsgol, Bulgan, and Arkhangay Provinces (Aimags). The northern part of the area is extremely steep with Khovsgol Mountains, that is 2,200 to 3,351 m above the sea level, while the southern part mostly consists of smooth hills where vast steppe develops.

Conifers called "taiga" vegetate widely in the area where it is chilly and covered with snow and ice for a long period in winter. Since the image analysis covers a large entire area and it is difficult to obtain effective data through optical sensors under such a climatic environment, we employed a SAR (Synthetic Aperture Radar) of JERS-1.

Eleven digital mosaic images were used for the analysis, each of which covers 1° (N-S) by 1.5° (E-W) with the reduced scale of 1:200,000.

2.2.2 Method of analysis

Division of geological unit and interpretation of geological structure including lineaments were conducted for the analysis. For division of geological unit, criteria described below were established to interpret photogeological features of the radar image. Then characteristic features were divided into some types in terms of each criterion, and geological unit was assigned to each of the types.

(1) Photographic features

- Color tones : dark, dark gray, gray and light gray
- Texture : coarse, intermediate and smooth

(2) Topographical features

- Drainage pattern: dendritic, parallel, semi-dendritic, semi-parallel and linear

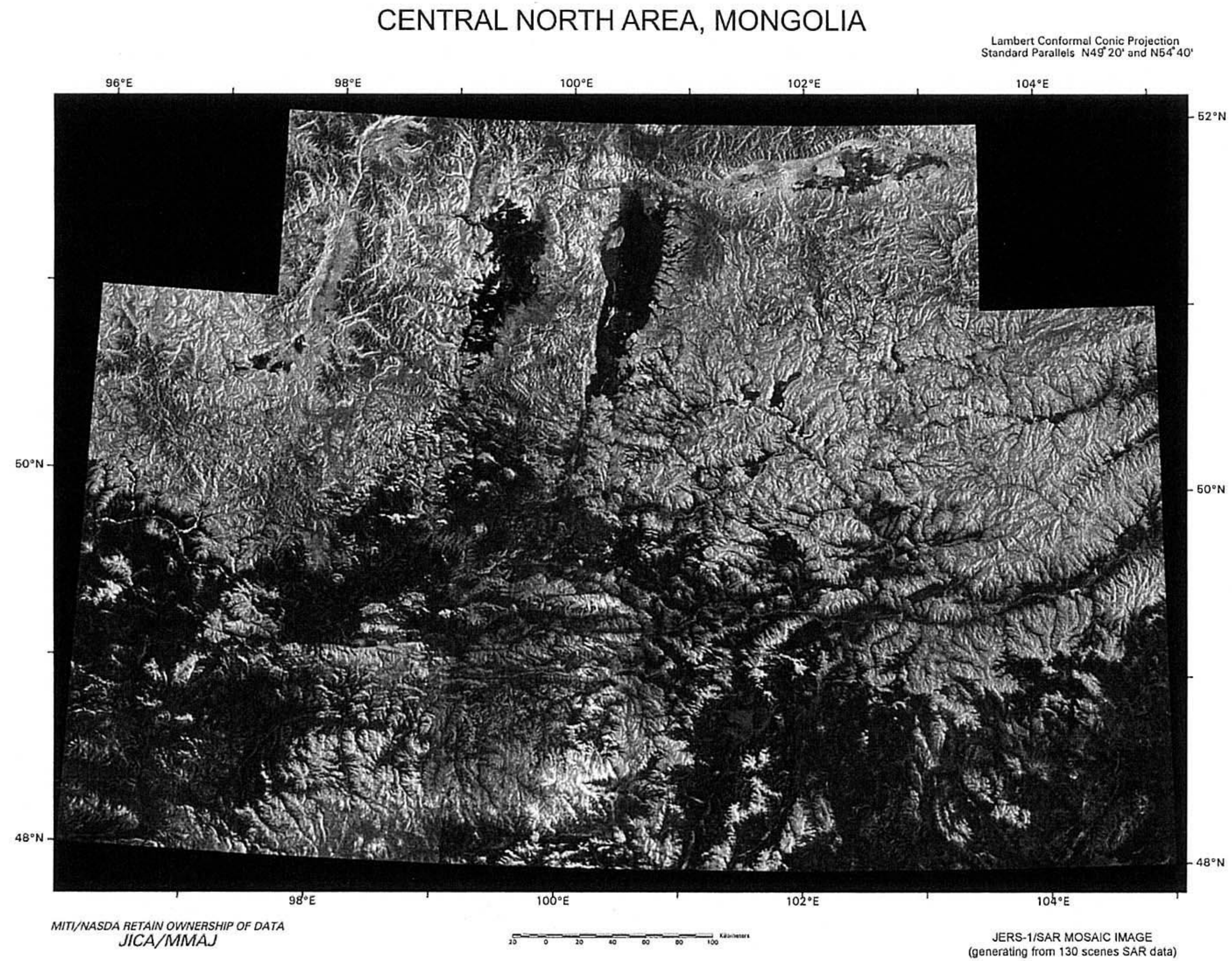

Fig.II-2-7 JERS-1/SAR mosaic image of the central-north area, Mongolia

- Drainage density: high, intermediate, low and extremely low
- Resistance: high, intermediate, low and extremely low
- Shape of ridge: sharp, round and flat
- Development of beddings: Clear, unclear and massive

2.2.3 Results of analysis and interpretation

(1) Division into geological units

In dividing the area into geological units based on the results of interpretation, we compared our interpretation results with the existing geological division referring to the existing geological maps of 1:500,000 scale, and decided names of geological units in accordance with symbols of the strata and rocks used in the geological map. Photographic and topographic features of individual geological units are shown in Table II-2-3a and Table II-2-3b respectively.

Division of geological unit was determined mainly on the basis of topographical features. Since a variety of vegetation is involved in the area such as coniferous forests, steppes, swamps, naked land, etc., photographic features shown in the radar images are almost attributable to difference in densities of vegetation (trees in particular). In other words, as radar waves scatter much on the land where trees grow closely together, the land is shown in bright tones on the image. On the other hand, since radar waves scatter little on steppes and naked land, the land is shown in dark tones on the image.

Resistance and drainage density to which we attached the greatest importance in the interpretation are described as follows:

(a) Resistance

Resistance means a degree of resistance of strata and rocks against erosion.

The geological units with high resistance formed a high land, because it shows high coefficient of permeability of strata and rocks due to high porosity and developed fractures into which infiltration of rainwater is large and small quantity of rain flow on the land surface. Therefore, the degree of erosion is low. However, in the geological units with low resistance, much rain flows on the land surface because of low coefficient of permeability. This causes excessive erosion, and a low land is formed.

Typical examples of the rocks with high resistance are coarse sandstone, conglomerates, limestone and granites with few fractures. Typical rocks of the units in this area are acidic volcanic rocks of the Permian (Plv (h)), sedimentary rocks of the Carboniferous (C1, C2), metamorphic rocks of the Proterozoic (R2, R3, PR1, AR2-PR1), granites of the early Palaeozoic (γ PZ1) and granitic gneisses (γ PR1).

On the other hand, typical rocks with low resistance are mudstone, fine grain tuff, sedimentary rocks, etc., while typical rocks of the units in this area are unconsolidated sediments and basalt lava of the Quaternary (Q2-Q5, N1) and sedimentary rocks (J1-2, J3-K1, K1) of the Jurassic to the Cretaceous.

(b) Drainage density

Like resistance described to above, drainage density also has a close relation with quantity of

Table II-2-3a Characteristics of photogeologic units (sedimentary and volcanic rocks)

Characteristics of Photogeologic Units (sedimentary and volcanic rocks)

(1)

Unit	Photo-characteristics		Morphologic Expression					Comparison with existing map	
	Tone	Texture	Drainage Pattern	Drainage Density	Rock Resistance	Ridge Type	Bedding	Geologic Unit	Geologic Age and Main Lithology
Q5	dark to medium grey	rough	colinear	very low	very low	flat	none	Q, βQ	Quaternary: sand,gravel,clay basalt
Q4	dark to light grey	smooth	meandering, anastomotic sub-dendritic	low	very low	flat	none	QⅣ, (QⅢ-Ⅳ)	Quaternary: sand,gravel,clay
Q3	dark	smooth	colinear	very low	very low to low	flat	none	QⅢ-Ⅳ, QⅢ	Quaternary: sand,gravel,clay
Q2	dark	smooth	colinear	very low	very low to low	flat	none	QⅡ-Ⅲ	Quaternary: sand,gravel,clay
N1	dark grey to medium grey	medium to rough	sub-dendritic	low	moderate	flat	(lava flow band)	βN1, βN2	Quaternary(Pliocene): trachy-basalt,basalt
K1	dark grey to medium grey	smooth	sub-dendritic, sub-parallel	medium	low	sharp(wide)	unclear	K1	Cretaceous: conglomerate, sandstone,mudstone
J3-K1	dark to medium grey	smooth	sub-parallel	low	low	sharp(tight)	rare	J3-K1	Jurassic to Cretaceous: conglo-merate,sandsone
J1-2	medium grey to dark grey	smooth	sub-parallel	low	low	round	unclear	J1-2, J1-2sh	Jurassic: conglomerate,sand-stone,mudstone
T3-J1	dark grey to medium grey	medium	sub-dendritic	medium	low to moderate	sharp(wide)	partly bedded	T3-J1mg	Triassic to Jurassic: andesite basalt,tuff
T2-3	dark grey to medium grey	medium	sub-parallel	medium	moderate to high	sharp(wide)	unclear	T2-3, T2-3ab1～4	Triassic: sandstone,conglo-merate,siltstone
P2-T1	medium grey to light grey	rough	sub-dendritic	low to medium	high	subround to sharp(tight)	unclear	P2-T1hr3	Permian to Triassic: trachy-basalt,trachyandesite
P2v	dark grey to medium grey	medium to rough	dendritic	high	low to moderate	sharp(tight)	massive	P2hr4	Permian: trachybasalt, trachyandesite
P2	medium grey	medium	sub-parallel	medium	high	round	unclear	P2	Permian: conglomerate,sand-stone,siltstone
P1v(h)	dark to medium grey	rough	dendritic	high to medium	moderate to high	sharp(tight)	massive	P1-2hn2+3, P1hn2, P1hn1, P1-2hn3	Permian: rhyolite,dacite,ande-site,basalt,tuff,sandstone
P1v(l)	dark to medium grey	rough	dendritic	high to medium	low	sharp(tight)	massive	P1-2hn2+3, P1hn2, P1hn1, P1-2hn3	Permian: rhyolite,dacite,ande-site,basalt,tuff,sandstone

Table II-2-3a Characteristics of photogeologic units (sedimentary and volcanic rocks)

Characteristics of Photogeologic Units (sedimentary and volcanic rocks)

(2)

Unit	Photo-characteristics		Morphologic Expression					Comparison with existing map	
	Tone	Texture	Drainage Pattern	Drainage Density	Rock Resistance	Ridge Type	Bedding	Geologic Unit	Geologic Age and Main Lithology
C2	medium grey	medium	sub-dendritic, sub-parallel	medium	high	sharp(wide)	partly bedded	C2ar	Carboniferous: sandstone, conglomerate
C1	medium grey	smooth	sub-dendritic	low	high	round	unclear	C1	Carboniferous: conglomerate, sandstone,siltstone
C1ur	dark to medium grey	medium	sub-dendritic	low to medium	low to moderate	sharp(wide) to round	partly bedded	C1ur1, C1ur2	Carboniferous: siltstone,conglomerate,sandsote
D	medium grey	rough	sub-dendritic, sub-parallel	low to medium	high	subround to sharp(wide)	unclear	D	Devonian: conglomerate,sandstone,tuff,siltstone
D1-2	medium grey	smooth	sub-dendritic	low	high	round	unclear	D1-2	Devonian: siltstone,sandstone conglomerate
S-D1	medium grey	rough	sub-dendritic	medium	moderate	sharp(wide)	unclear	S-D1, S-D1hr	Silurian to Devonian: andesite dacite,rhyolite,tuff
€3-O	medium grey	rough	dedritic	low to medium	high	round	unclear	€3-O	Cambrian to Ordovisian: shale siltstone,phyllite,sandstone
€2-O1 (h)	medium grey	medium	sub-dendritic	high	moderate to high	sharp(tight)	unclear	€2-O1	Cambrian to Ordovisian: sandstone,siltstone,phyllite,shale
€2-O1 (l)	medium grey	medium	sub-dendritic, sub-parallel	very high	low	sharp(tight)	unclear	€2-O1	Cambrian to Ordovisian: sandstone,siltstone,phyllite,shale
€1	medium grey to light grey	rough	sub-dendritic	high	moderate to high	subround to sharp(wide)	unclear	€1,€1br, V-€1hs, V-€1, V-€1eg	Cambrian: limestone,dolomite
R3	medium grey	rough	sub-dendritic	medium	high	subround to sharp(wide)	partly bedded	R3, R3-V	Proterozoic: dolomite,quartzite limestone
R2	medium grey	rough	sub-dendritic	low to medium	high	subround to sharp(tight)	partly bedded	R2	Proterozoic: metaeffusive rocks metatuff,metasandstone
PR1	medium grey to light grey	rough	sub-dendritic	medium	high	sharp(wide)	unclear	PR1	Proterozoic: shale,amphibolite marble
AR2-PR1	medium grey to light grey	rough	sub-dendritic	low	high	sharp(wide) to round	unclear	AR2-PR1	Proterozoic: gneiss,amphibolite marble

Table II-2-3b Characteristics of photogeologic units (intrusive rocks)

Characteristics of Photogeologic Units (intrusive rocks)

(1)

Unit	Photo-characteristics		Morphologic Expression					Comparison with existing map	
	Tone	Texture	Drainage		Rock Resistance	Ridge Type	Bedding	Geologic unit	Geologic Age and Main Lithology
			Pattern	Density					
γJ	medium grey to dark grey	rough	sub-parallel	high	moderate	sharp(tight)	none	γJ	Jurassic: granite,granite porpyry,diorite,granodiorite
γT3-J1	medium grey to dark grey	medium	sub-dendritic	low	moderate	sharp(wide)	none	γT3-J1	Triassic to Jurassic: granite, granodiorite
πγP2-T1	medium grey to dark grey	medium	sub-dendritic	low	low	round	none	πγP2-T1	Permian to Triassic: granite porphyry,plagioporphyry
γP2-T1	medium grey to light grey	rough	sub-dendritic	high	high	sharp(wide)	none	γP2-T1, γεP2-T1	Permian to Triassic: granite, granodiorite,gabbro
γP2	medium grey	rough	sub-dendritic	high	moderate to high	sharp(tight)	none	γP2	Permian: monzonite,syenite monzosyenite,granodiorite
εγP	light grey	rough	sub-dendritic	medium	high	subround	none	εγP	Permian: alkaline granite, syenite,granosyenite
γP	dark to medium grey	medium	sub-dendritic, sub-parallel	medium	low to high	round	none	γP	Permian: granite,granodiorite
γδC2-3	medium grey	rough to smooth	sub-dendritic	medium	high to moderate	sharp(tight) to sharp(wide)	none	γδC2-3, γC2-3	Carboniferous: granite,grano-diorite,diorite,gabbro
εPZ2	medium grey	rough	sub-parallel	high	high	sharp(tight)	none	εPZ2	Middle Paleozoic: syenite, nordmarkite,palascite
γD2	medium grey	medium	sub-dendritic	medium	moderate to high	subround to sharp(tight)	none	γD2	Devonian: granite,granosyenite
γδS	medium grey	rough	sub-dendritic	medium	high	sharp(wide)	none	γδS	Silurian: granodiorite
γS	dark	smooth	sub-parallel	low	low	sharp(tight)	none	γS	Silurian: granite,adamellite
γ-γδPZ1	light gry to dark grey	rough to medium	sub-dendritic	medium	high to low	sharp(tight)	none	γ-γδPZ1	Early Paleozoic: granite, granodiorite,diorite
γPZ1	medium grey to light grey	rough	dendritic	medium	high	sharp(tight)	none	γPZ1	Early Paleozoic: biotite granite, plagiogranite

Table II-2-3b Characteristics of photogeologic units (intrusive rocks)

Characteristics of Photogeologic Units (intrusive rocks)

(2)

Unit	Photo-characteristics		Morphologic Expression					Comparison with existing map	
	Tone	Texture	Drainage		Rock Resistance	Ridge Type	Bedding	Geologic unit	Geologic Age and Main Lithology
			Pattern	Density					
$\gamma\delta$PZ1	light grey	medium	sub-dendritic	medium	high	round to subround	none	$\gamma\delta$PZ1	Early Paleozoic: adamellite, granodiorite, tonalite
$\nu\delta$PZ1	medium grey	rough	sub-dendritic	medium	moderate to high	sharp(tight) to subround	none	$\nu\delta$PZ1	Early Paleozoic: gabbro, gabbroic diorite, diorite
σR3-Є1	medium grey	rough	sub-parallel	medium	high	round	none	σR3-Є1	Riphean to Cambrian: dunite, harzburgite, wehrlite
γR	light grey to dark	rough	sub-dendritic	medium	high	subround	none	γR	Riphean: leucocratic granite, gneissose granite
$\nu\delta$PR	light grey to dark	medium	sub-dendritic	low	high	subround	none	$\nu\delta$PR	Proterozoic: anorthosite, gabbroic anorthosite
γPR1	medium grey	medium	sub-dendritic	low to medium	high	sharp(tight)	(schistose)	γPR1	Proterozoic: granitic gneiss, migmatite, granite

rainwater flowing on the land surface. The more rain flows on the land surface, the more drainage are developed, and in case smaller amounts of rain flow on the land surface, drainage density becomes lower. In general, therefore, while the geological units with high drainage density tend to have low resistance, those with low drainage density tend to have high resistance. However, as an exceptional case, in unconsolidated and loose strata like sedimentary rocks of the Quaternary, both drainage density and resistance are low.

Rocks existing in geological units with high drainage density are basalts of the Permian (P2v), sedimentary rocks of the Cambrian to Ordovician (C2-01(h), C2-01(1)) and granites of the Permian to Ordovician (γ P2, γ P2-T1), etc.

On the other hand, rocks existing in geological units with low drainage density are unconcolidated sediments and basalt lava of the Quaternary (Q2-Q5, N1), sedimentary rocks of the Jurassic (J1-2), metamorphic rocks of the Proterozoic (AR2-PR1), granitic gneisses of the Proterozoic (γ PR1), etc.

(2) Analysis and interpretation of geological structures

During interpretation and analysis of geological structures, we extracted lineaments and circular structures. Out of the lineaments extracted, those which can be identified on the image as faults and those drawn as faults in the existing geological maps were determined to be faults and shown in the interpretation map.

(a) Lineament

There is a difference between lineaments extracted from the valley of the Selenge river which flows to the east in the center and those extracted from the districts to the north and south of the valley.

In the central part, distinctive E-W lineaments which continues well were dominant, and short NW-SE lineaments were additionally noted. In the northern part of the valley where extraction density was low, short lineaments of the NW-SE and E-W trends were identified. In the southern part of the valley, lineaments of the NW-SE and N-S trends were dominant, and extraction density was high especially in the southeastern part.

In every place described above, lineaments of the NW-SE trend were identified. These lineaments intensively occur in the images ranging from the Bulgan 1:200,000 Sheet area which is located in the southeastern part of the survey area, through the southern part of Lake Khuvsgul situated in the northeastern part of the area, to the south of the lake in a width of approximately 200 km, diagonally crossing the E-W lineament in the central part.

(b) Circular structure

The following circular structures below were identified in the area. It was interesting that circular structures extracted from the western part of the Jarganant sheet area and the southeastern part of the Hutag sheet area might have been formed by intrusion of small-scaled rocks and have accompanied alteration zones.

[Central part of the Erdenebulgan sheet area]

A circular structure having a diameter of 2 km was extracted from an area where granitic rocks of the early Proterozoic (γ δ PZ1) occur.

[Northern part of the Rashaant sheet area]

A circular structure having a diameter of 4 km was extracted from an area where a stratum of the Cambrian (C1) occur.

[Northern part of the Ingettolgoy sheet area]

A semi-circular structure having a diameter of 15 km was extracted from an area where gneiss of the Proterozoic (AR2-PR1) occur.

[Western part of the Jarganant sheet area]

A circular structure having a diameter of 10 km was extracted from an area where alkali granites of the Permian (γ P2) occur, and a caldera-like concave was identified in its central part.

[Southeastern part of the Hutag sheet area]

A circular structure having a diameter of 15 km was extracted from an area where acid volcanic rocks of the Permian (Plv (1)) occur, and existence of a lineament traversing in the E-W trend was identified in its central part. There is a conial depression at the center of the circular structure.

Figure II-2-8 shows a radar image around the circular structures described in western part of the Jarganant sheet area and southeastern part of the Hutag sheet area.

2.2.4 Distribution of mineral occurrences

Figure II-2-9 shows distribution of mineral occurrences of gold, copper and molybdenum which is based on the existing data before this survey and plotted on the mosaic image. From this figure, distribution of mineral occurrences is summarized as follows:

(1) Gold

Mineral occurrences of gold are located in the northeastern end, northern central part and the southeastern end of the area. In the northern central part of the area, every Au occurrence accompanies Cu mineralization.

(2) Copper

Mineral occurrences of copper are located not only in the entire district of the southern part, but also in the central part along with the NW-SE lineaments.

(3) Molybdenum

Mineral occurrences of molybdenum are located accompanied with copper mineralization. Other occurrences were scattered all over the area.

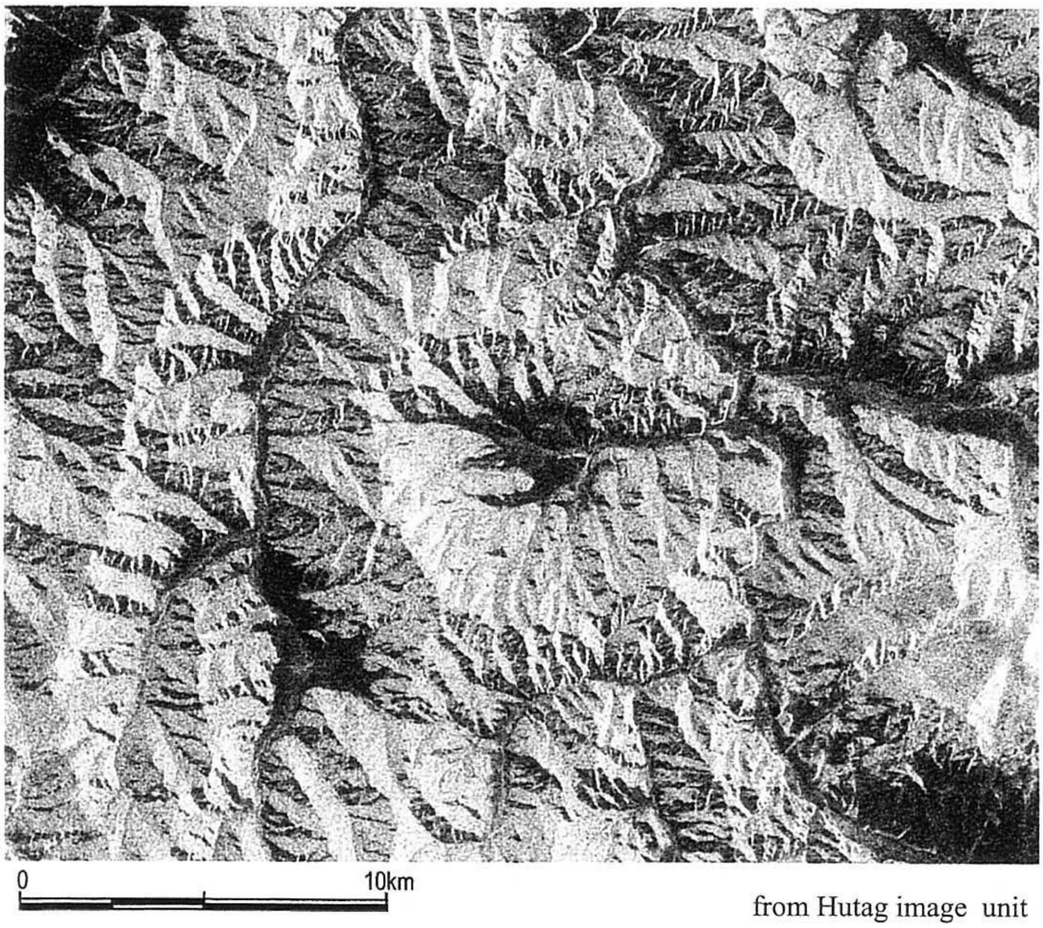

from Hutag image unit

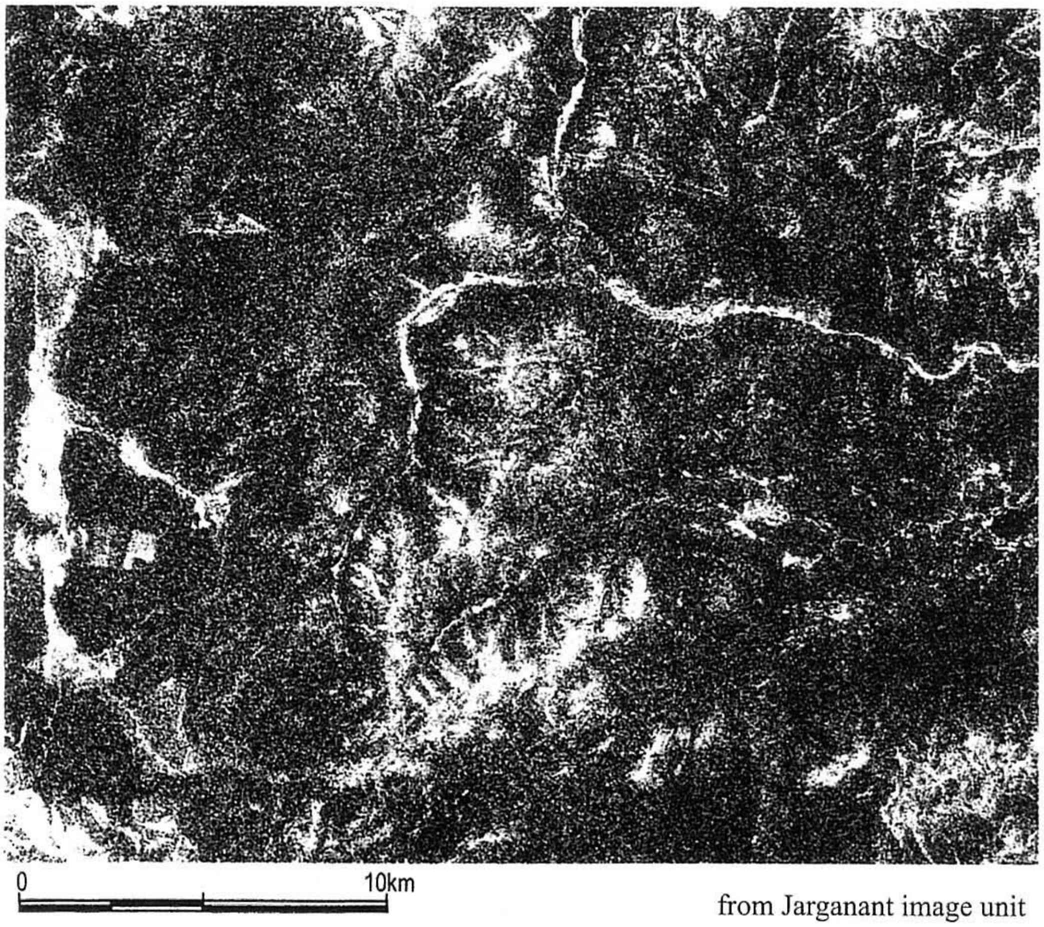

from Jarganant image unit

Fig.II-2-8 Circular structures from JERS-1/SAR mosaic images analysis

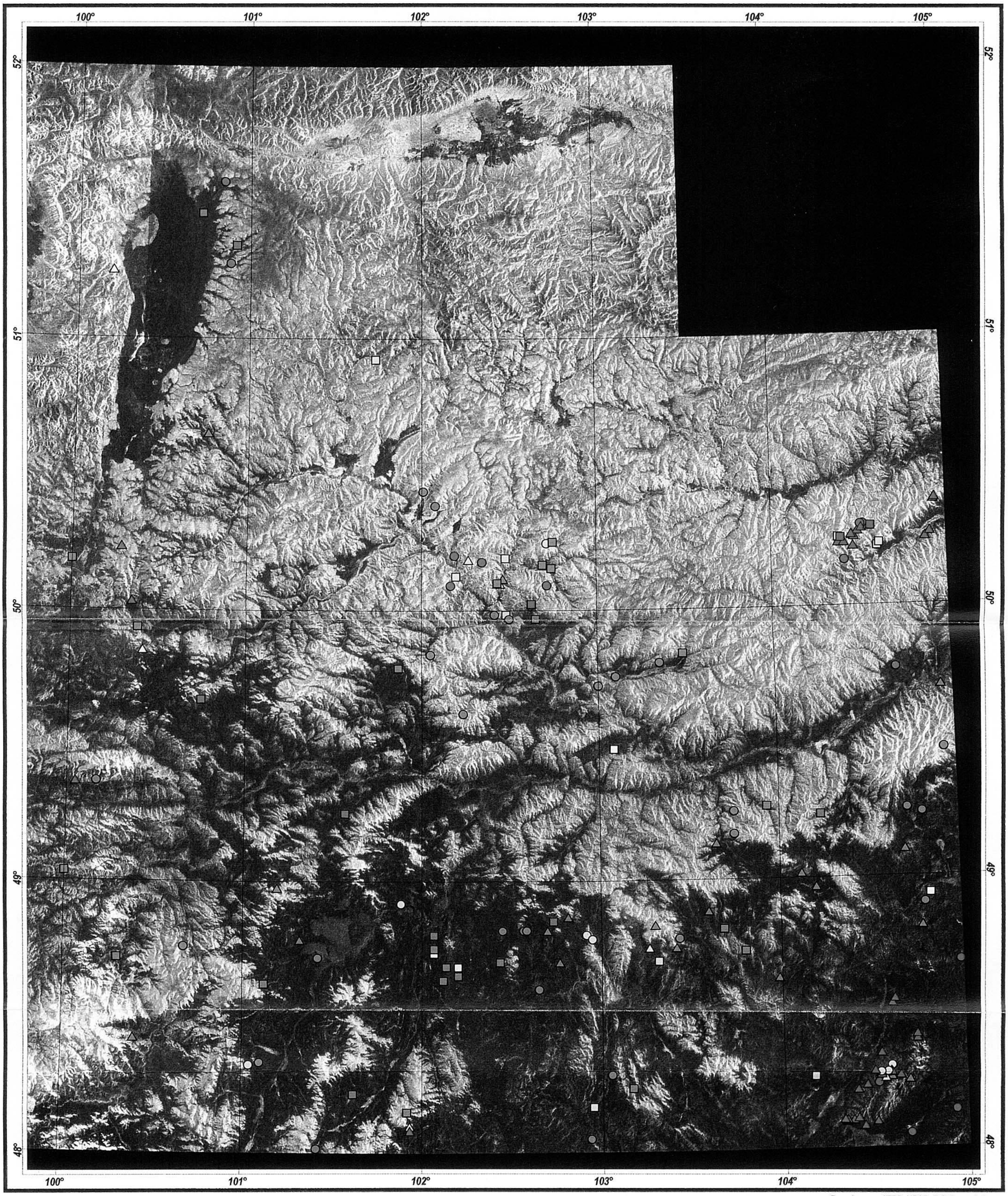

Base image : JERS-1/SAR digital mozaic image

LEGEND

Minerals
- Au
- Au + Cu
- Cu
- Cu + Mo
- Mo
- Au + Mo

Type
- ○ Alteration
- □ Stockwork, Quartz Vein
- △ Fracture, Scarn, Greisen, Others

50 0 50 km

Fig.II-2-9 Distribution of mineral occurrences on JERS-1/SAR mosaic images

2.2.5 Summary

Figure II-2-10 shows a mosaic image on which locations of lineaments, circular structures and mineral occurrences are indicated. Through comparison of the image analysis and interpretation with the existing mineral occurrences, the following two sites were extracted as targets to be surveyed.

- Southern part of Lake Khuvsgul and zone ranging from its south to southeastern part of theBulgan 1:250,000 Sheet area, where the NW-SE lineaments are dominant:
  Principal targets of the area are porphyry copper deposit and vein type gold and/or copper deposit. In this zone, two places, i.e. surroundings of the Egiyn River in the central part and the southeastern part of the Hutag 1:250,000 Sheet area, where a circular structure was extracted, are considered to be especially promising.

- A district in the western part of the Jarganant 1:250,000 Sheet area where a circular structure was identified:
  Copper showing has already been known in its vicinity. Because this circular structure exists on a hill and caldera-like concave is observed in its central part, occurrence of small-scaled stocks which accompany alteration zones is expected.

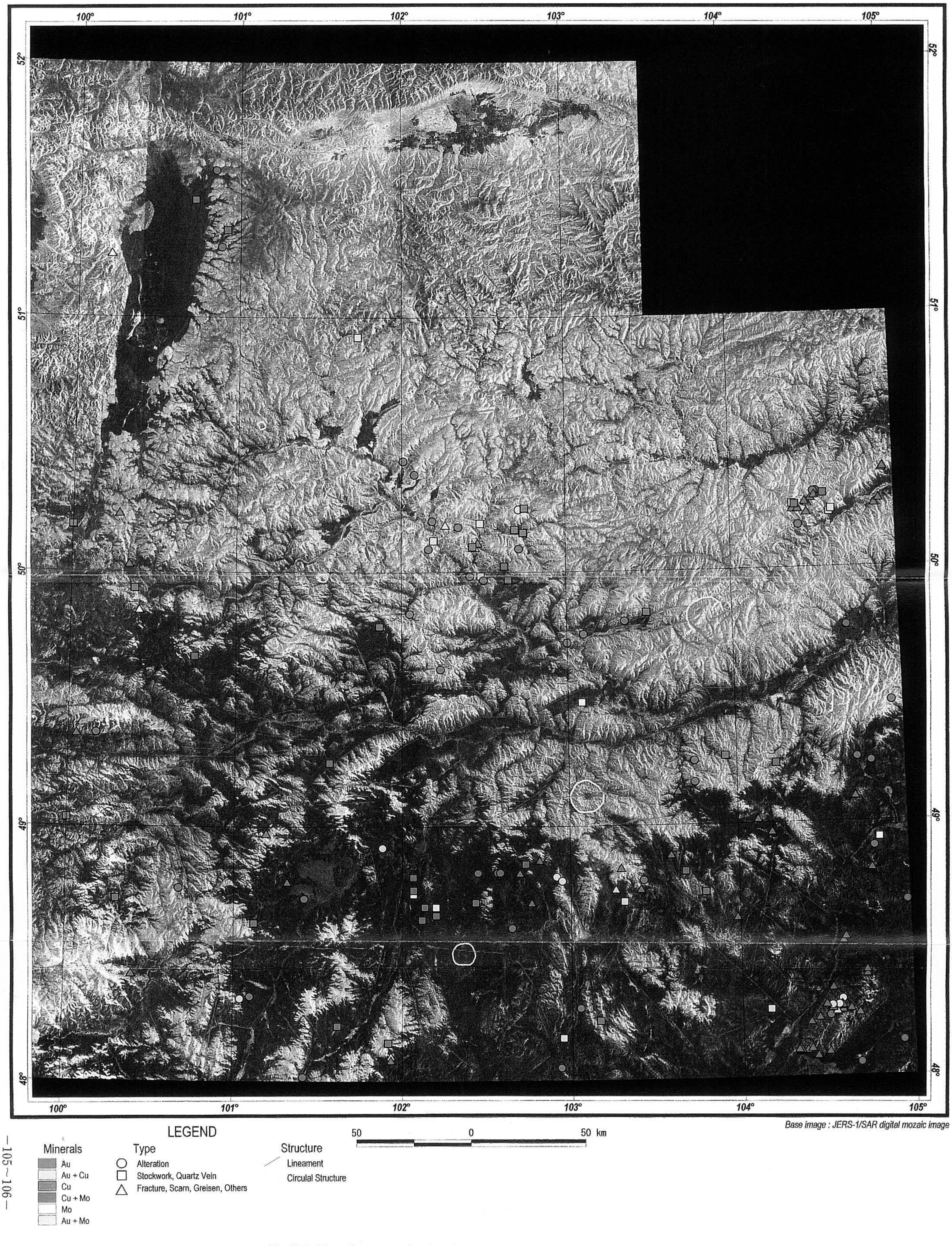

Fig.II-2-10 Interpretation based on JERS-1/SAR mosaic images analysis